

Permanent wilting point plays an important role in simulating winter wheat growth under water deficit conditions

Ning Yao^{a,b,1}, Yi Li^{b,1}, Fang Xu^a, Jian Liu^b, Shang Chen^b, Haijiao Ma^b, Henry Wai Chau^c, De Li Liu^d, Meng Li^a, Hao Feng^{a,e}, Qiang Yu^{a,e}, Jianqiang He^{a,b,*}

^a State Key Laboratory of Soil Erosion and Dryland Farming on the Loess Plateau, Institute of Soil and Water Conservation, Northwest A&F University, Yangling, 712100, Shaanxi, PR China

^b Key Laboratory for Agricultural Soil and Water Engineering in Arid Area of Ministry of Education, Northwest A&F University, Yangling, 712100, Shaanxi, PR China

^c Department of Soil and Physical Sciences, Faculty of Agriculture and Life Science, Lincoln University, Lincoln, Canterbury, 7647, New Zealand

^d NSW Department of Primary Industries, Wagga Wagga Agricultural Institute, Wagga Wagga, NSW, 2650, Australia

^e Institute of Soil and Water Conservation, Chinese Academy of Science and Ministry of Water Resources, Yangling, 712100, Shaanxi, PR China

ARTICLE INFO

Keywords:

Winter wheat
Water stress
Permanent wilting point
CERES-Wheat
DSSAT

ABSTRACT

Soil parameters related to soil water holding capacity could play an important role in simulating winter wheat growth under severe soil water stress, which could heavily influence the simulated soil water contents, and then biomass and final yield. In this study, a field experiment of winter wheat (*Triticum aestivum* L.) was conducted in two consecutive growing seasons (2012–2014) under rainfall shelter in arid areas of China, with the purpose to identify to what extent the soil parameters could influence the simulated output variables in the DSSAT-CERES-Wheat model under water stress conditions. The permanent wilting point (PWP), which were initially indirectly measured based on soil sampling, were manually tuned through a trial-and-error method based on field observations of soil water content and aboveground biomass. The results showed that the maximum advancing of maturity date was about five days under water stress conditions. The stages of returning green and grain-filling were critical periods for agricultural water management of winter wheat in arid areas. The relative mean absolute error (RMAE) of simulated and observed variables were almost all less than 20% when water stress occurred at the heading and grain-filling stages. However, there were relatively large simulation errors when water stress occurred at the wintering and returning green stages. In addition, the CERES-Wheat model did not correctly simulate the discrepancies in phenology dates of winter wheat. The overall averaged root mean square error of all treatments for total water storage in 0–100 cm soil layer and winter wheat biomass decreased to 0.3 mm and 750 kg ha⁻¹ after manually tuning the initially indirectly measured value of PWP. In general, the CERES-Wheat model showed some limitations to simulate winter growth under complicated arid conditions. Meanwhile, the measurement uncertainty in soil parameter PWP could introduce large simulation errors in simulating crop growth response to severe water stress conditions. We suggest the soil parameter PWP should be more carefully calibrated based on relevant field observations since it is related to crop type and difficult to be directly and precisely measured. In general, it is necessary to further research into the responding mechanism and simulation of winter wheat growth to water stress in liable-drought areas.

1. Introduction

Winter wheat (*Triticum aestivum* L.) is one of the main staple crops in arid and semi-arid regions of the Northwest China. However, winter wheat production is constrained by increasingly tight water supplies (Shan et al., 2002). Therefore, it is of great significance to define the

growth response of winter wheat under different water stress periods and develop water-saving measures for the sustainable production of winter wheat in this region.

Water stress at different growth stages could have different kinds of influences on crop phenology and yields (Angus and Moncur, 1977; Kang et al., 2002; McMaster and Wilhelm, 2003). The reduction of final

* Correspondence author at: Key Laboratory for Agricultural Soil and Water Engineering in Arid Area of Ministry of Education, Northwest A&F University, Yangling, 712100, Shaanxi, PR China.

E-mail address: jianqiang_he@nwsuaf.edu.cn (J. He).

¹ These authors contributed equally to this work.

yield is related not only to the intensity of water stress, but also to crop growth stage (Cakir, 2004; Wang et al., 2004). The stages of returning green and grain-filling were critical periods for agricultural water management of winter wheat in arid areas. Therefore, it is necessary to clarify the critical periods of water demand for agricultural water management of winter wheat in arid areas. Typically, this kind of research usually depends on traditional field plot experiments, whereas the results are usually site-specific and may not be sufficiently extrapolated.

Crop growth simulation models (or crop models) can predict crop yield based on environmental conditions and agricultural managements. They are widely used to analyze the influential factors on the agricultural system, help find the optimal management practices, and provide technical guidance for decision support for farmers and decision makers (Antle et al., 2016; Jones et al., 2016). Crop growth simulation models are typically defined as mathematical representations of the reactions that occur within the plant and the interactions between the plant and its environment (Hammer et al., 2006). The interactions within plant could include growth, development, photosynthesis, assimilate partitioning, and yield formation. The interactions might include unpredictable inputs (future daily weather), predictable inputs (soil parameters), and interventions (e.g. planting date, irrigation, and application of fertilizer). It is a multidisciplinary platform for agronomic research, which involves plant physiology, ecology, agronomy, agricultural meteorology, and plant nutrition fertilizer science (Hammer et al., 2006; Jones et al., 2003).

So far, main wheat growth simulation models include STICS (Brisson et al., 1998), AFRCWHEAT2 (Porter et al., 1993), CERES-Wheat (Ritchie and Otter, 1985), Sirius (Jamieson et al., 1998), SU-CROS2 (van Laar et al., 1992v), and SWHEAT (van Keulen and Seligman, 1987v), etc. The CERES-Wheat model, a widely used wheat growth simulation model in the world, has been applied in many types of application, such as irrigation scheduling, fertilizer management, and influences of climate change on wheat production (Attia et al., 2016; Dettori et al., 2011; Thorp et al., 2010). For example, He et al. (2013) applied the CERES-Wheat model to simulate the growth and development of spring wheat under different irrigation conditions in Minqin County, Gansu province of China. An optimal irrigation schedule was brought forward based on the results of model simulations. In previous studies, the CERES-Wheat model has also been used to simulate soil water dynamics (Eitzinger et al., 2004) and wheat yields (Biernath et al., 2011) under water stress conditions. However, there were some limitations for the CERES series model to simulate crop growth under water stress conditions. For example, Nouna et al. (2003) found that the values of leaf area index (LAI), biomass, and grain yield of maize were all underestimated under serious water stress. This limitation was caused by the inaccurate estimation of evapotranspiration (ET) under water stress, which was also confirmed in the simulations with CERES-Maize model (Dejonge et al., 2011). Thus, further research is needed to improve the CERES series model to simulate wheat growth under water stress at different growth stages.

It is very important to determine properly the soil parameters related to total available water, which represented soil water holding capacity, to correctly simulate ET during the growing season (Campos et al., 2016). Total available water depended on effective root depth and the difference between soil water contents at field capacity and wilting point (Campos et al., 2016). However, it is usually difficult and expensive to directly measure the soil water content at permanent wilting point (Ghorbani et al., 2017; Rab et al., 2011), which might heavily affect the simulation accuracy of CERES-Wheat model.

However, most of the studies focused on the estimation of genetic coefficients, or crop related parameters, while soil parameters were generally directly measured in the experiment. Unfortunately, direct measurements of soil parameters were usually difficult and expensive (Mohanty et al., 2015). Therefore, soil parameters were often estimated through indirect methods, such as class pedotransfer functions (Wösten

et al., 1995), multiple linear regression (Minasny et al., 1999), extended nonlinear regression (Scheinost et al., 1997), and artificial neural network (Pachepsky et al., 1996). These indirect methods would introduce uncertainties in soil parameters and then in the simulated output variables. Unfortunately, it is still not clear how large the simulation errors introduced by soil parameters could be in the simulation of winter wheat growth with the CERES-Wheat model.

In this study, we used the experimental data of winter wheat growth under water stresses at different growth stages in two consecutive years (2012–2014) to analyze the influences of intensity and occurring stage of water stress on the growth and yield of winter wheat in arid areas of Northwest China. The objectives were (1) to study the response of winter wheat growth to water stress at two adjacent stages and explore the optimal irrigation dates and quotas; (2) to evaluate the reliability of the CERES-Wheat model to simulate winter wheat growth and yield under different scenarios of water stress; and (3) to identify to what extent the soil parameters could influence the simulated output variables in the CERES-Wheat model when under severe water stress conditions. This study will provide a basis for scheduling deficit irrigation for winter wheat based on the CERES-Wheat model and also promote the application of CERES-Wheat model in other relevant studies of agro-ecological system in arid and semi-arid regions of China.

2. Materials and methods

2.1. Experimental site description

The field experiments were conducted in the Irrigation Station of the Northwest A&F University (34°17'N, 108°04'E, 506 m) from 2012 to 2014 at Yangling, Shaanxi province, China. This area belongs to semi-arid regions in China with a typical temperate and monsoonal climate. Temporal distribution of local precipitations was uneven, which makes it prone to develop seasonal droughts. The long term average annual frost-free days, temperature, sunshine, and precipitation were 221 d, 12.9 °C, 2196 h and 660 mm, respectively. The soil type of the experimental site was *Lou* soil (silt loam), with a pH of 8.14, total organic carbon content of 8.20 g kg⁻¹, and total nitrogen of 0.62 g kg⁻¹ in the 0–20 cm soil layer.

2.2. Field experiments

The winter wheat cultivar involved was 'Xiaoyan 22', a popular wheat cultivar planted in the Guanzhong Plain where the experimental site is located. The planting dates were Oct. 15th both in 2012 and 2013. Dry wheat seeds were sown in drill, with a planting depth of 5–6 cm, row spacing of 25 cm, and planting density of 4 × 10⁶ plant ha⁻¹. The harvest dates were Jun. 2nd in 2013 and Jun. 7th in 2014. The level of fertilization application was the same for all treatments, with a base fertilizer of 140 kg N ha⁻¹ and 50 kg P₂O₅ ha⁻¹ but without top dressing. A representative quadrat of 1 m² was randomly selected and marked in each plot to determine the final yield, which must not be disturbed during the whole growing season. Regular soil and plant sampling (with three replicates) should be conducted outside the square.

The experimental factors were irrigation level and water-stress period. The water requirements of winter wheat in the whole growth period were about 400–500 mm in this region. This experiment was designed to have full irrigation treatment with a total amount of 400 mm irrigation as commonly practiced in the region. There were two levels of reduced irrigation treatments, i.e., 120 mm and 240 mm of total irrigation. As we investigated the scenarios of two consecutive stages without irrigations within the five stages of wheat cropping season, there were four possible irrigation schedules for each level of water stresses (see Table 1). Therefore, three irrigations of 40 mm and 80 mm each time were available for the reduced irrigation treatments of 120 mm and 240 mm, respectively. The whole growing season of winter

Table 1

. Treatments in the experiment of water stresses at different stages of winter wheat. The exact dates of irrigation events were listed in the parentheses in 'mm-dd' format. The unit of irrigation was mm.

Treatment	Wintering (12/15)	Returning green (03/15)	Jointing (04/15)	Heading (05/01)	Gain- filling (05/ 15)	Total irrigation depth
CK	80	80	80	80	80	400
I1D1	0	0	40	40	40	120
I1D2	40	0	0	40	40	120
I1D3	40	40	0	0	40	120
I1D4	40	40	40	0	0	120
I2D1	0	0	80	80	80	240
I2D2	80	0	0	80	80	240
I2D3	80	80	0	0	80	240
I2D4	80	80	80	0	0	240

wheat was divided into five different stages (i.e. wintering, returning green, jointing, heading, and grain-filling). Phenology was documented using the Zadoks scale (Zadoks et al., 1974). For example, when the occurrence rate of jointed winter wheat was up to 50%, this day was known as jointing stage. Water stress occurred at an individual stage might have relatively limited influences, but water stress occurred at two adjacent stages might have more serious damage on wheat growth. Thus, each water-stress period included two adjacent growth stages, i.e. wintering + returning green (D1), returning green + jointing (D2), jointing + heading (D3), and heading + grain-filling (D4). Consequently, there were a total of eight treatments, with three replicates for each of them (Table 1). A total of 24 plots following a split-plot experimental design were arranged under a giant movable rainout shelter to exclude the influences of rainfall on experiments. The area of each plot was 8 m². Adjacent plots were separated by polyethylene plastic films buried 1.5 m below soil surface to prevent subsurface water flow. Additionally, a check treatment (CK) was arranged nearby, which also had three replicates. The irrigation method was border irrigation. Experimental design was the same for both two growing seasons.

2.3. CERES-Wheat model description

The CERES-Wheat model in the Decision Support System for Agrotechnology Transfer (DSSAT) software, is specific for the simulation of wheat growth (Jones et al., 2003). It was embedded in the DSSAT-CSM (Cropping system model) platform and was able to call the common modules of soil water, nitrogen and carbon balances, and the meteorological and soil databases. The CERES-Wheat model simulates the development, growth, yield, and carbon and water balances at a daily step (Jones et al., 2016, 2003). The processes simulated include solar radiation interception and photosynthesis of canopy, nutrient uptake and activity of roots, assimilate partitioning, water uptake and transpiration, growth and respiration, leaf area expansion, organ genesis and senescence, field management, etc. The data required for running CERES-Wheat model usually include four types: weather data, soil data, crop genetic coefficients, and management information.

In the DSSAT model, daily soil water balance was simulated with the one-dimensional 'tipping bucket' method (Ritchie, 1985, 1998). Vertical soil water movement and root water uptake could be simulated for each soil layer. Potential water uptake was a function of root length density, depth, distribution, and actual soil water content. Potential evapotranspiration (ET) could be calculated either with the Priestley-Taylor method (Priestley and Taylor, 1972) or with the FAO56 Penman-Monteith method (Allen et al., 1998). Potential crop ET was a function of crop leaf area index (LAI) and ET₀. DSSAT implemented water stress factors of TURFAC (Eq. 1) and SWFAC (Eq. 2) to simulate the crop growth and development as followed (Anapalli et al., 2008).

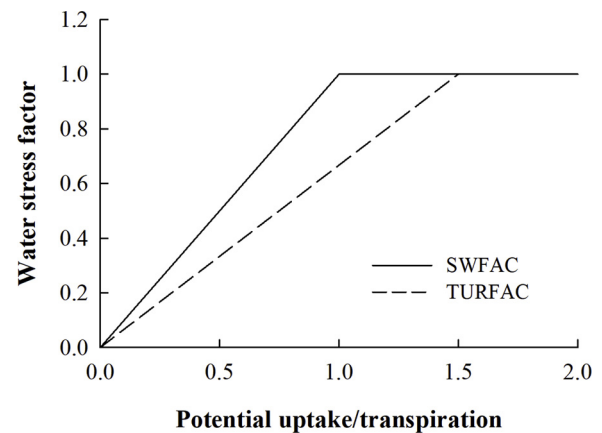


Fig. 1. Relationship used to calculate water stress factors SWFAC and TURFAC in the DSSAT model (from Ritchie, 1998).

$$TURFAC = \frac{TRWUP}{RWUEP_1 \times EP_0} \quad (1)$$

$$SWFAC = \frac{TRWUP}{EP_0} \quad (2)$$

where *TURFAC* is the first water stress or turgor factor; *TRWUP* is potential root water uptake; *EP₀* is the potential transpiration, and *RWUEP₁* is a species-specific parameter that is currently set to 1.5 for all DSSAT crops.

Under well-watered conditions, potential root water uptake is higher than potential transpiration. As the soil dries out because of root water uptake and surface evaporation, potential root water uptake decreases. At a certain stage, a threshold is reached where the first water stress or turgor factor (*TURFAC*, Eq. 1) is activated (Fig. 1). This level of water stress is mainly implemented to modulate expansive growth, which in many cases is more sensitive to drought stress than the other growth and development processes. When potential transpiration demand equals or exceeds the potential root water uptake, a second stress factor (*SWFAC*, Eq. 2) is activated (Fig. 1) (Ritchie et al., 1998). The water stress factor *SWFAC* mainly affects growth and biomass related processes. For winter wheat, a drought stress might accelerate the development rate and shorten the days to flowering, seed set, or physiological maturity, but it might decelerate the development rate for some other crops. Under non-stress conditions, both factors are set to 1.0. Once the stress factors have been activated, they decrease to a value less than 1 proportionally to the severity of difference between potential transpiration demand and potential extractable soil moisture

2.4. Data for model application

2.4.1. Weather data

Daily weather data of 2012–2014 were obtained from the National General Weather Station at Yangling, which was about 100 m away from the experimental site. The daily data included sunshine hour (h), maximum temperature (°C), minimum temperature (°C), and precipitation (mm) (Fig. 2). The values of precipitation were set to 0.0 mm since the experiment was conducted under the rainout shelter. Daily solar radiation was estimated based on sunshine hours and the Angstrom equation (Eq. 3) (Angstrom, 1924).

$$R_s = R_{max} \left(a_s + b_s \frac{n}{N} \right) \quad (3)$$

where *R_s* is the daily total solar radiation, MJ m⁻²; *R_{max}* is the daily extraterrestrial solar radiation on a horizontal surface, MJ m⁻²; *n* is the daily sunshine hours, h; *N* is the day length, h; *a_s* and *b_s* are two empirical coefficients, which are related to atmospheric conditions and set as 0.25 and 0.50 as recommended by the Food and Agriculture

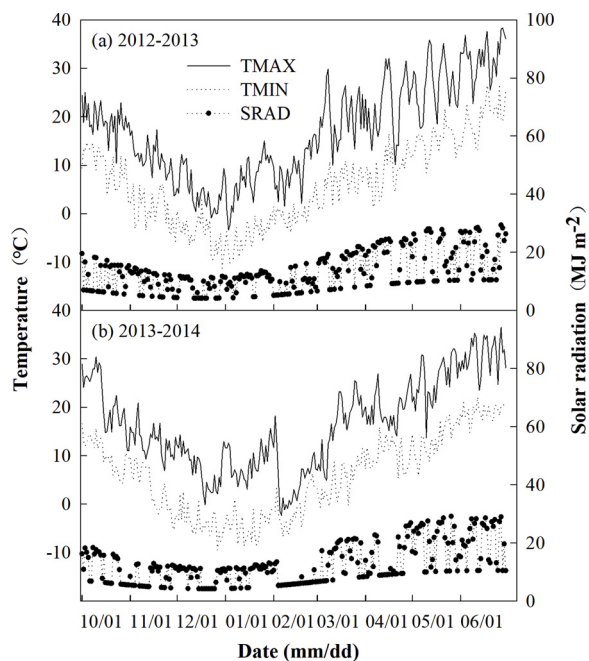


Fig. 2. Daily temperatures and solar radiation during the 2012–2013 (a) and 2013–2014 (b) growing seasons of winter wheat in Yangling, Shaanxi province, China. TMAX, TMIN, and SRAD represent daily maximum temperature, minimum temperature, and solar radiation, respectively.

Organization (FAO).

2.4.2. Soil data

Soil physical properties of each layer were measured directly before the experiment. Soil texture was analyzed with the laser particle size analyzer (TopSizer, Zhuhai OMEC Instruments Co., Ltd., China). The parameters of permanent wilting point and field capacity were measured through an indirect method based on high-speed centrifugation. First, the cutting-ring method was used to collect soil sample for each 20-cm layer to a depth of 100 cm. Next, each soil sample was soaked more than 48 h until completely saturated. Third, the high-speed centrifugation was used to obtain soil water content and soil water potential. Fourth, the RETention Curve software in HYDRUS 2 was used to fit the van Genuchten retention function (van Genuchten, 1980v). Finally, the values were derived indirectly for soil parameters of permanent wilting point (soil water contents at -1500 kPa), field capacity (soil water contents at -10 kPa), and saturation (soil water contents at 0 kPa) based on the retention function above. However, the parameter of permanent wilting point was influenced by crop species, soil type, and crop stage of growth (Norton and Silvertooth, 1998). This indirect measurement method would introduce uncertainties in its value and then in the simulated model output variables. Therefore, permanent wilting point was then manually tuned again through a trial-and-error method based on field measured soil water content.

Table 2

Genetic coefficients of winter wheat in the CERES-Wheat model and their estimated values for the cultivar of 'Xiaoyan 22' investigated in this study.

Parameter	Definition	Estimated value
P1V	Days, optimum vernalizing temperature, required for vernalization (d)	58.03
P1D	Photoperiod response (% reduction in rate/10 h drop in pp) (%)	91.90
P5	Grain filling (excluding lag) phase duration (°C d)	604.6
G1	Kernel number per unit canopy weight at anthesis (# g ⁻¹)	22.64
G2	Standard kernel size under optimum conditions (mg)	41.72
G3	Standard, non-stressed mature tiller weight (incl grain) (g)	1.002
PHINT	Interval between successive leaf tip appearances (°C d)	130

To measure soil water moisture, soil samples were collected randomly at representative crop-covering points in the plots with an auger at every 20 cm throughout a depth of 1.0 m. The soils collected were mixed and then dried in an oven at a constant temperature of 105 °C for 24 h. The volumetric soil water moisture was obtained by the multiplication of mass soil water moisture and soil bulk density. The sampling frequency was once in two weeks before the jointing stage, and then once a week thereafter.

2.4.3. Crop growth data

As mentioned above, a quadrat of 1 m² was randomly selected and marked after emergence to represent the average growth status and determine the final yield of winter wheat in each plot. For plant sampling, a total of five representative plant samples of winter wheat were randomly collected outside the quadrat. The plants were dried in an oven at a temperature of 75 °C for 48 h to a constant weight. Then the dry matter weights were measured to determine the aboveground biomass. The plant sampling frequency was as the same as soil sampling. After physiological maturity, all of the wheat plants in each quadrat were harvested. The dry matter biomass was measured as above. The number of productive ears was counted. The average grain number per ear was measured based on ten representative ears. Finally, all of the sampled ears were threshed. The grains were also dried in an oven at a constant temperature of 75 °C for 48 h. Dry-matter grain yield and 1000-kernel weight (or unit grain weight) were then measured with an electronic scale.

2.5. Model calibration and verification

The generalized likelihood uncertainty estimation (GLUE) is a Bayesian method for parameter estimation (Beven and Binley, 1992; He, 2009; He et al., 2010). The GLUE method assumed that, in the case of large models with many parameters, there was no exact inverse solution. Hence, the estimation of a unique set of parameters, which optimized a goodness-of-fit criterion given the observations, was not possible. The main principle of this method was to discretize the parameter space by generating many parameter values from the prior distribution. Likelihood values were then calculated for each parameter set using field observations. Probabilities, an empirical posterior distribution of the parameters, were calculated using Bayes' equation (Romanowicz and Beven, 2006).

The GLUE approach is implemented as a package for automatic parameter estimation in DSSAT. The fact that it was used to estimate the genetic coefficients related to the Chinese winter wheat cultivar 'Xiaoyan 22' must come later (Table 2). There were two rounds of model runs in current DSSAT-GLUE package. Genetic coefficients related to crop phenology were estimated in the first round, while coefficients related to crop growth in the second. Main procedures in each round of GLUE included: (1) set-up of prior distributions for genetic coefficients; (2) generation of random parameter sets from the prior distributions; (3) model runs with the random parameter sets; (4) calculation of likelihood values; and (5) construction of posterior distributions. At least 3000 model runs were recommended in each round of GLUE to

ensure that the genetic coefficients were each estimated accurately and the posterior distributions were reliable (He, 2008).

However, the current DSSAT-GLUE program did not consider other parameters except for genetic coefficients related to crop cultivars. The soil parameters, especially those related to soil-water-holding capacity (e.g. saturation, field capacity, and PWP) were usually set as the measured values and seldom be estimated again. Whereas, we found the PWP, which is heavily dependent on crop types, played an important role in simulating soil water contents and final yield under soil water stress. Thus, this parameter had to be carefully estimated. Unfortunately, there is no such an automatic tool available to estimate the soil parameters. Therefore, PWP was manually tuned again through a trial-and-error method based on the comparisons between the simulated and measured soil water contents in different soil layers. The CERES-Wheat model was then evaluated twice based on the indirectly measure and manually tuned soil parameters, respectively.

In this study, we used four kinds of model output and observation variables for parameter estimation and model verification, including phenology (anthesis and maturity dates), unit grain weight, final biomass, and grain yield. The data from the non-stressed CK treatment in the two growing seasons were used for model calibration. A final set of genetic coefficients was obtained after 20,000 models runs in each round of GLUE (Table 2). Then, the data from other rest treatments were used for model verification, in which the measurements and simulations of concerned output variables were compared.

2.6. Statistical analysis

Two statistics of relative mean absolute error (RMAE) and relative root mean square error (RRMSE) between simulated and observed output variables were used to evaluate the results of model calibration and verification. Both statistics were able to measure the discrepancy between model simulations and field observation. Additionally, they were dimensionless and could be used for the comparison between different output variables. Usually, lower values of RMAE and RRMSE indicate higher accuracy of model simulation.

$$RMAE = \frac{1}{n} \sum_{i=1}^n \frac{|S_i - O_i|}{|O_i|} \times 100\% \quad (4)$$

$$RMSE = \sqrt{\frac{1}{n} \sum_{i=1}^n (S_i - O_i)^2} \quad (5)$$

$$RRMSE = \frac{RMSE}{\bar{O}} \times 100\% \quad (6)$$

where S_i is the i -th simulated variable; O_i is the i -th observed variable; \bar{O} is the mean value of observations; and n is the number of variables.

3. Results

3.1. Influences of different irrigation scenarios on winter wheat growth and yield

3.1.1. Influences on plant heights

Different irrigation scenarios had no remarkable influences on plant heights of winter wheat under the irrigation level of I1 (Fig. 3a), but there was some difference under I2 (Fig. 3c). Generally, the treatments of D3 (water stress at jointing and heading stages, 2012–2013 season) and D4 (water stress at heading and grain-filling stages, 2013–2014 season) had the highest height, while D1 (water stress at wintering and returning green stages) had the shortest height. It can be concluded that irrigations at early vegetative growth stages could to some extent increase plant height of winter wheat. Larger irrigation amounts might lead to more increment. This kind of trend was more obvious in the field experiment of 2013–2014 (Fig. 3b and 3d). Either under irrigation I1 (Fig. 3b) or I2 (Fig. 3d), treatments of D4 (water stress at heading and

grain-filling stages) and D3 (water stress at jointing and heading stages) had relatively similarly higher plant heights, while treatments of D2 (water stress at returning green and jointing stages) and D1 (water stress at wintering and returning green stages) shared relatively similarly shorter plant heights. The comparisons above proved that irrigation at the returning green stage could remarkably increase the plant height of winter wheat, in other words, improve the vegetative growth of winter wheat.

Compared with the CK treatments in the two seasons, all treatments had shortened plant heights (Fig. 3). Plant heights increased slowly after returning green, and then increased rapidly until the heading stage. For instance, it took about 130 days for winter wheat to grow from emergence to a height of 15 cm. The average growth rate was only about 0.12 cm d^{-1} . However, it took only about 50 days from 15 cm to 75 cm, with an average growth rate of 1.2 cm d^{-1} , or about ten times of the former rate. Plant heights of 'Xiaoyan 22', the winter wheat cultivar investigated in this study, kept 70–80 cm after heading stage or 180 days after planting.

3.1.2. Influences on winter wheat biomass

The above-ground biomass values of all treatments were lower than those of CK treatments in the 2012–2013 growing season (Fig. 4a and 4c). There were no obvious differences among the treatments for their biomass under irrigation level of I1, but treatment related to D1 (water stress at wintering and returning green stages) had slightly lower biomass than the other treatments when under I2. However, the situation was more complicated in the 2013–2014 growing season. Compared with the CK treatment, all treatments had lower biomass in the 2013–2014 growing season (Fig. 4c and 4d). When under irrigation level of I1 (except CK), treatments related to D1 (water stress at wintering and returning green stages) had the lowest biomass and followed by D2 (water stress at returning green and jointing stages), while treatments related to D3 (water stress at jointing and heading stages) and D4 (water stress at heading and grain-filling stages) shared the similarly highest biomass. When under I2 (except CK), the biomass of treatments related to D1 (water stress at wintering and returning green stages) were remarkably lower than the other treatments, while there were no great differences among the treatments related to D2 (water stress at returning green and jointing stages), D3 (water stress at jointing and heading stages), and D4 (water stress at heading and grain-filling stages). Like plant height, above-ground biomass of all treatments showed similar growth pattern in both two seasons. The biomass grew very slowly before jointing stage (about 150 days after planting), then increased rapidly until arriving at its maximum at the maturity stage.

3.1.3. Influences on winter wheat phenology

Different irrigation scenarios investigated in this study all had some influence on winter wheat phenology dates to varying degrees in both 2012–2013 and 2013–2014 seasons. In the 2012–2013 season, main phenology dates were almost the same for all treatments before the jointing stage, without significant difference (Fig. 5a; $P < 0.05$). However, later phenology dates (e.g. heading, anthesis, grain-filling, and maturity) changed significantly ($P < 0.05$) due to different irrigation scenarios. For treatment IID1, the later phenology dates were all earlier than the other treatments since the total irrigation was only 120 mm in the whole season and water stress occurred continuously in the wintering and returning green stages. The maximum advancing of maturity date was about five days. Under the same irrigation level (I1 or I2), the heading and anthesis dates of D1, D2, D3, and D4 were delayed one to three days, respectively. Generally, the heading and anthesis dates advanced more if water stress occurred earlier. Irrigation levels also had some influences on phenology dates. The treatments related to irrigation level I1 were generally one to three days earlier than those related to I2 for their heading and anthesis dates. It confirmed the phenomenon that serious water stress could bring forward

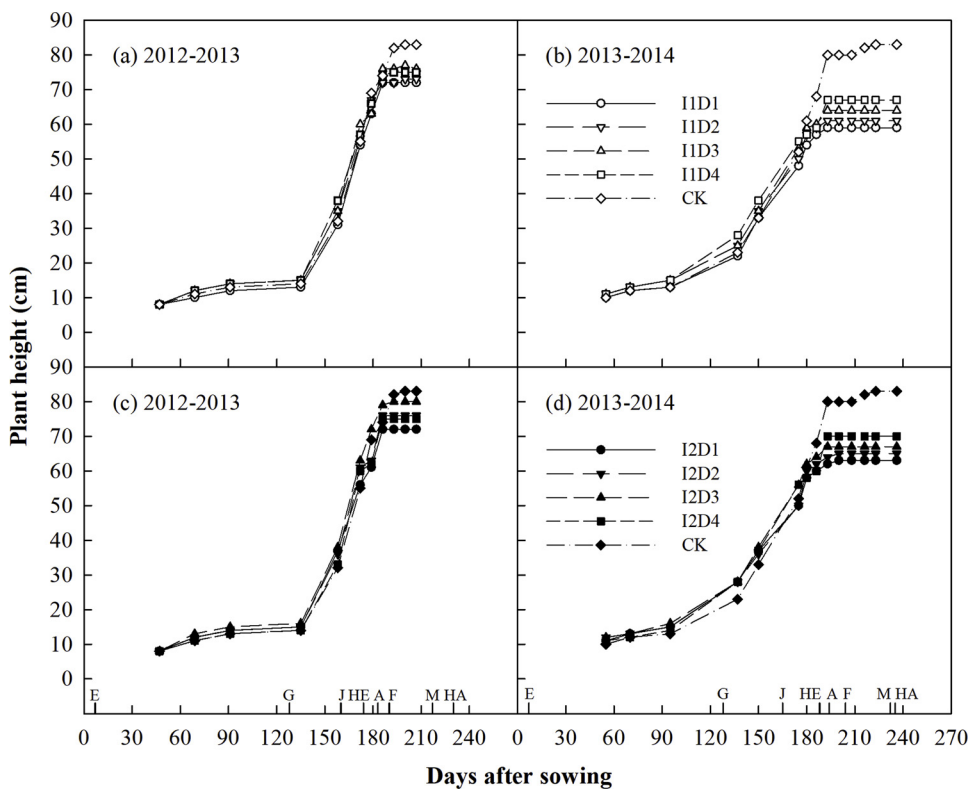


Fig. 3. Plant heights of winter wheat at different growth stages under different irrigation scenarios in the two growing seasons of 2012–2013 (a, c) and 2013–2014 (b, d). The letters E, G, J, HE, A, F, M and HA represent the different growth stages of emergence, returning green, jointing, heading, anthesis, filling, maturity, and harvest, respectively. I1 and I2 represent the two irrigation levels and D1–D4 the four different periods of water stress (Table 1). The same as below (For interpretation of the references to colour in this figure legend, the reader is referred to the web version of this article).

the phenology dates before anthesis to various degrees. For the CK treatment, the heading, anthesis, grain-filling, and maturity dates were all later than those of the other treatments in the 2012–2013 season. The maximum difference between heading dates could be as large as nine days (Fig. 5a). The same phenomena were also observed in the 2013–2014 season.

3.1.4. Influences on winter wheat yields

Different irrigation scenarios obviously influenced the yield components and grain yields of winter wheat both in the 2012–2013 and 2013–2014 seasons (Table 3). When under irrigation level of I1 in the 2012–2013 season, the numbers of productive ears and grains per ear of treatments related to D3 (water stress at jointing and heading stages)

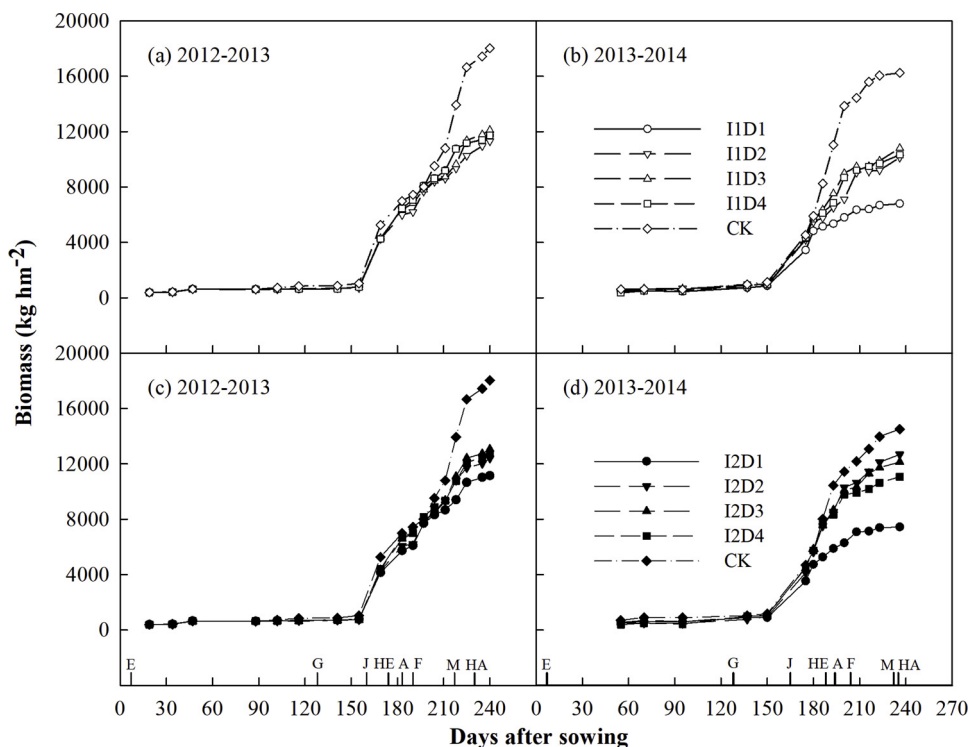


Fig. 4. Aboveground biomass accumulation of winter wheat at different growth stages under different irrigation scenarios in the two growing seasons of 2012–2013 (a, c) and 2013–2014 (b, d).

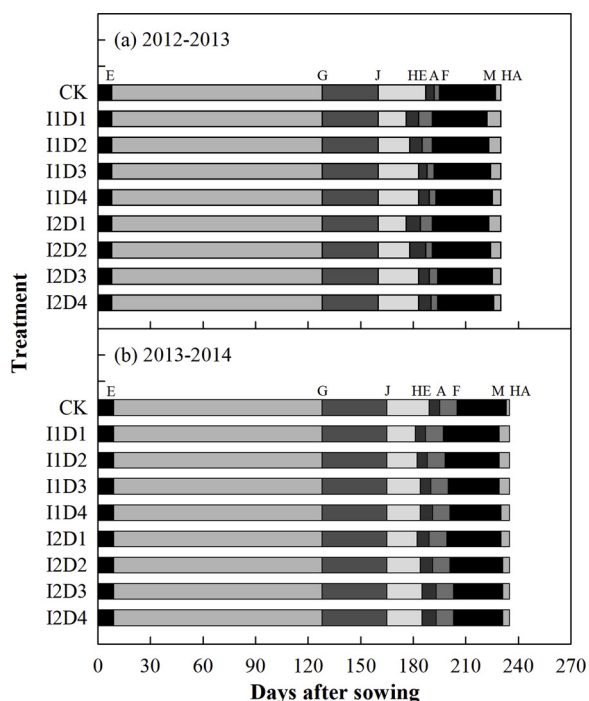


Fig. 5. Development stages of winter wheat under different irrigation scenarios in the two growing seasons of 2012–2013 (a) and 2013–2014 (b).

and D4 (water stress at heading and grain-filling stages) were all higher than those related to D1 (water stress at wintering and returning green stages) and D2 (water stress at returning green and jointing stages). However, the values of 1000-kernel weight were lower than those related to D1 and D2. Generally, treatments related to D1 and D2 showed no great difference for their yields and yield components, as well as D3 and D4. Hence, it could be concluded that returning green was the critical irrigation stage for productive ears, grains per ear, and final yield, while heading was the critical irrigation stage for 1000-kernel weight of winter wheat. Treatments of I1D3 and I1D1 obtained the maximum and minimum grain yields, respectively. The same phenomena were also observed under the irrigation level of I2.

Compared with the 2012–2013 season, the experimental results of 2013–2014 were different to some extent since the values of productive ears, grains per ear, and final yields of almost all treatments were lower than the last season. This was because the soil water contents were relatively low before sowing in the 2013–2014 season, which led to insufficient water available for the vegetative growth before jointing stage. Both under I1 and I2, the values of productive ears, grains per

Table 3

Influences of water stress at different growth stages on the growth and yields of winter wheat in the two growing seasons of 2012–2013 and 2013–2014. In the same season, values with different letters within each column are significantly different at $\alpha = 0.05$ and $n = 3$ plots for the same irrigation level.

Treatment	2012–2013				2013–2014			
	Productive ears (10^4 hm^{-2})	Kernels per ear	1000-kernel weight (g)	Gain yield (kg hm^{-2})	Productive ears (10^4 hm^{-2})	Kernels per ear	1000-kernel weight (g)	Grain yield (kg hm^{-2})
CK	676.50	38	36.20	8407	617.00	30	47.23	7488
I1D1	562.67 b	33 b	33.73 a	5079 d	453.33 b	22 c	44.27 a	2927 b
I1D2	557.67 b	31 c	33.28 a	5202 c	455.00 b	23 c	43.31 a	4375 a
I1D3	679.33 a	37 a	27.06 b	5626 a	491.33 a	25 b	41.42 b	4440 a
I1D4	670.67 a	38 a	26.84 b	5316 b	491.67 a	27 a	40.40 b	4168 ab
I2D1	580.33 c	33 b	36.99 a	5755 d	451.00 b	24 c	45.71 a	3503 c
I2D2	598.67 bc	34 b	34.51 a	6682 a	466.00 b	26 b	46.10 a	5243 a
I2D3	675.33 a	36 a	27.84 b	6460 b	518.67 a	30 a	43.89 b	4884 b
I2D4	652.33 ab	36 a	27.75 b	6323 c	520.67 a	31 a	43.10 b	4733 b

Note: Because a split-plot experimental design was used in this study, but the CK treatment was not involved in this design. Therefore, the statistical analysis of split-plot experiment did not include the CK treatment.

ear, and 1000-kernel weight of treatments related to D3 (water stress at jointing and heading stages) and D4 (water stress at heading and grain-filling stages) were close to each other, but all higher than those related to D1 (water stress at wintering and returning green stages) and D2 (water stress at returning green and jointing stages). This trend agreed with the experimental results of 2012–2013 seasons. Either under I1 or I2, the treatments related to D1 (water stress at wintering and returning green stages) all gave the lowest yields, or only 66% and 67% of the highest yields obtained by I1D3 and I2D2.

3.2. Simulation of winter wheat growth and yield under different irrigation scenarios

3.2.1. Model calibration and verification

With the GLUE-estimated genetic coefficients (Table 2) and indirectly measured soil parameters (Table 4), the simulated and observed anthesis and maturity dates were almost the same, with relative mean absolute error (RMAE) of only 0.52% and 0.21% for the model calibration process (Table 5). The simulation accuracy of biomass and grain yield was also high with RMAE values of 6.48% and 4.22%, whereas the accuracy of unit weight simulation was relatively low with an RMAE of greater than 10%. For the model verification process, the simulation accuracy of anthesis and maturity dates was 2.09% and 2.20%. However, the simulated anthesis and maturity dates were exactly the same for different treatments in each year, while observed dates were different because of various water stress scenarios. The simulation accuracy of unit grain weight, biomass, and grain yield was relatively poor. Especially for the treatments with water stress at heading and grain-filling stages, the RMAE values of output variables concerned were all greater than 20%. In contrast to grain yield, biomass was poorly simulated when water stress occurred at returning green stage. For example, the RMAE values of treatment related to D1 (water stress at wintering and returning green stages) and D2 (water stress at returning green and jointing stages) were all greater than 30% and 20%, respectively. This indicated that water stress before jointing could have great influences on model simulation of biomass and grain yield. Generally, the values of overall average RMAE and RRMSE were all about 5% for the calibration processes and above 15% for the calibration processes.

3.2.2. Comparisons of time-series output variables under indirectly measured soil parameters

The CERES-Wheat model was run with the indirectly measured soil parameters (i.e. permanent wilting point and field capacity), GLUE-estimated genetic coefficients, and the relevant input data of 2012–2013 growing season. The simulated dynamics of winter wheat biomass and soil water contents were compared among different

Table 4
Initial soil properties of the experimental site of winter wheat experiment in 2012–2013 and 2013–2014 seasons.

Soil layer (cm)	Clay (%)	Silt (%)	Bulk density (g cm ⁻³)	Field capacity (cm ³ cm ⁻³)	Saturated water content (cm ³ cm ⁻³)	Permanent wilting point (cm ³ cm ⁻³)		Initial water content (cm ³ cm ⁻³)	
						Measured	Estimated	2012–2013	2013–2014
0–20	18.36	42.29	1.26	0.25	0.43	0.15	0.12	0.23	0.20
20–40	19.45	43.65	1.35	0.31	0.45	0.16	0.16	0.24	0.21
40–60	17.4	42.83	1.30	0.27	0.44	0.16	0.14	0.26	0.18
60–80	16.09	41.99	1.32	0.29	0.35	0.14	0.13	0.27	0.18
80–100	16.36	42.35	1.35	0.29	0.35	0.15	0.14	0.29	0.21

Note: the content of clay and silt were volume percent.

treatments (Figs. 6–8). Roots of winter wheat mainly concentrated in the 0–80 cm soil profile. And the 0–40 cm soil layer usually contained the majority of the root lengths and had a large root length density (Wang et al., 2006). In addition, soil water contents of 0–20 cm layer changed greatly and had a great potential influence on crop growth. Thus, only the soil water dynamics of 0–20 cm layer was presented for the sake of brevity.

When sufficient irrigation was applied, the dynamics of winter wheat biomass and soil moisture of CK treatment could all be accurately simulated (Fig. 6). During the 2012–2013 and 2013–2014 growing seasons, the determination coefficient (R^2) and root mean square (RMSE) between simulation and observation of biomass were 0.98, 0.97 and 1,144, 1,490 kg ha⁻¹, respectively. And they were 0.45, 0.81 (R^2) and 0.05, 0.03 cm³ cm⁻³ (RMSE) for soil moisture in the 0–20 cm layer. Generally, the simulation accuracy of biomass was higher than soil moisture (Fig. 6a), but the main trend of soil water dynamics was correct since most simulations matched the corresponding observations (Fig. 6b). Thus, it could be concluded that the CERES-Wheat model was able to correctly simulate the dynamics of winter wheat biomass and soil moisture when there was sufficient irrigation water.

However, when under different scenarios of soil water stress, the simulated dynamics of biomass and soil moisture varied greatly (Figs. 7 and 8). Either under I1 or I2, if there were continuous water stress at early vegetative stages (e.g. D1 and D2), there would be great errors in simulated biomass after jointing stage since simulations were lower than observations (Fig. 7a, b, e, and f). This indicated that the CERES-Wheat model overestimated the inhibition of winter wheat growth by soil water stress at returning green stage. With the delay of water stress, the simulation of winter wheat biomass gradually improved. If water stress occurred at the heading and grain-filling stages (D4), model simulated and observed results were close to each other (Fig. 7d and h). In this case, the CERES-Wheat was able to correctly simulate winter wheat growth with water stress at later growth stages.

For soil moisture at the 0–20 cm layer, the simulation errors would become larger with the increase of soil water stress. The simulation accuracies under irrigation level of I1 (Fig. 8a–d) were generally lower than those under I2 (Fig. 8e–h). When under the same irrigation level of I1, if water stress occurred at early stage of winter wheat growth, simulated soil moisture was usually lower than the observations. In other words, the model underestimated soil moistures at this stage or overestimated the level of soil water stress, which probably mainly contributed to the great errors in biomass simulation (Fig. 8a, b, e, and f). However, with the delay of water stress, the simulation accuracy of soil moisture gradually improved. When water stress occurred at the heading and grain-filling stages (D4), the simulations and observations matched very well (Fig. 8d and h), which confirmed once again that the CERES-Wheat model was able to correctly simulate soil water content when water stress occurred at later growth stages.

3.2.3. Comparisons of time-series output variables under manually tuned soil parameters

With the manually tuned soil parameters and GLUE-estimated

genetic coefficients, the simulated dynamics soil water contents (Simulated 2) were compared among different treatments at the 0–20 cm layer (Fig. 9). Through slightly adjusting the values of permanent wilting point and increasing field capacity (Table 4), the simulation accuracy was greatly improved for each treatment. Most simulated values matched the corresponding observations (Fig. 9). Thus, it was concluded that the CERES-Wheat model was able to correctly simulate soil moisture under different irrigation scenarios if the soil parameters related to water holding capacity could be correctly estimated.

To further verify the influences of soil parameters of permanent wilting point, the simulated dynamics of total water storage in the 0–100 cm soil profile (Fig. 10) and winter wheat biomass (Fig. 11) were compared among different treatments based on initial indirectly measured (Simulated 1) and new manually tuned soil parameters (Simulated 2). The simulation accuracies of total water storage were improved under both two irrigation levels after manually tuning the soil parameters (Fig. 10). The improved simulation accuracies were generally higher under I2 than those under I1. For each treatment, the simulation accuracy was improved obviously after 160 d (day after sowing). The general RMSE values decreased by 3.3, -0.1, -0.6, -1.0, 0.5, -0.4, 1.1, -0.7 mm for treatments I1D1, I1D2, I1D3, I1D4, I2D1, I2D2, I2D3, and I2D4 when compared to results simulated with initial indirect soil parameters and GLUE-based genetic coefficients, or Simulated 1, respectively. The overall mean RMSE of all treatments decreased to 0.3 mm. For different treatments, the simulation accuracies decreased or increased to different extents after changing the soil parameters. In addition, simulated total water storage was usually lower than the observations under the same irrigation level of I1. In other words, the model overestimated the level of soil water stress, which might contributed to the errors in biomass simulation.

Both under I1 and I2, the simulation accuracies of aboveground biomass were improved for almost all of the treatments after manually tuning the soil parameters (Fig. 11). The improved simulation accuracies under I2 were higher than those under I1. For each treatment, the simulation accuracies were improved obviously after 160 d (day after sowing), especially under irrigation level of I2. The general RMSE values decreased by 1475, 678, 363, 352, 1605, 1411, 645, -530 kg ha⁻¹ for treatments I1D1, I1D2, I1D3, I1D4, I2D1, I2D2, I2D3, and I2D4 when compared to the results of Simulated 1, respectively. The simulation accuracy of I2D4 became slightly lower after manually tuning the soil parameters. The overall mean RMSE value decreased 750 kg ha⁻¹. Thus, the simulation accuracy was improved greatly under different water stress conditions after manually tuning the soil parameters of permanent wilting point and field capacity.

4. Discussions

4.1. Influences of different irrigation scenarios on winter wheat growth

Different irrigation scenarios investigated in this study showed remarkable influences on plant height and aboveground biomass of

Table 5 Results of calibration and verification of the CERES-Wheat model based on indirectly measure soil parameters and GLUE-estimated genetic coefficients in simulating winter wheat growth under different scenarios of soil water stress. ARE is absolute relative error, %; Sim. and Obs. represent the simulated and observed values. The same as below.

Season	Treatment	Anthesis date (days after planting)		Maturity date (days after planting)		Unit grain weight (g)		Aboveground biomass (kg hm ⁻²)		Gain yield (kg hm ⁻²)	
		Obs.	Sim.	Obs.	Sim.	Obs.	Sim.	Obs.	Sim.	Obs.	Sim.
Model calibration	2012-2013 CK	192	190	228	228	0.036	0.040	18029	16531	8407	8131
	2013-2014 CK	196	196	235	236	0.047	0.040	16243	15516	7488	7874
Model validation	Average	184	190	222	228	0.034	0.040	11014	5783	5079	3161
	I1D1	185	190	223	228	0.032	0.040	11309	7413	5202	4188
	I1D2	188	190	224	228	0.027	0.030	12110	8795	5626	5136
	I1D3	188	190	225	228	0.027	0.024	11719	8942	5316	4876
	I1D4	184	190	223	228	0.037	0.040	12159	5784	5755	3161
	I2D1	187	190	224	228	0.035	0.040	13401	7376	6682	4107
	I2D2	189	190	225	228	0.028	0.029	13065	9486	6460	5443
	I2D3	190	190	226	228	0.028	0.034	12756	13287	6323	7411
	I2D4	188	196	229	236	0.043	0.040	6432	2664	2927	1433
	Average	191	196	229	236	0.043	0.039	9129	7486	4375	2931
2013-2014	I1D1	191	196	229	236	0.044	0.040	10011	8364	4440	5259
	I1D2	192	196	230	236	0.044	0.022	9264	8848	4168	4290
	I1D3	190	196	230	236	0.046	0.040	7438	2664	3503	1433
	I1D4	192	196	231	236	0.046	0.040	12684	10510	5243	4132
	I2D1	194	196	231	236	0.048	0.040	12130	11837	4884	6776
	I2D2	194	196	231	236	0.045	0.026	11066	12480	4733	5983
	I2D3	194	196	231	236	0.045	0.026	11066	12480	4733	5983
	I2D4	194	196	231	236	0.045	0.026	11066	12480	4733	5983
	Average	194	196	231	236	0.045	0.026	11066	12480	4733	5983
	Average	194	196	231	236	0.045	0.026	11066	12480	4733	5983

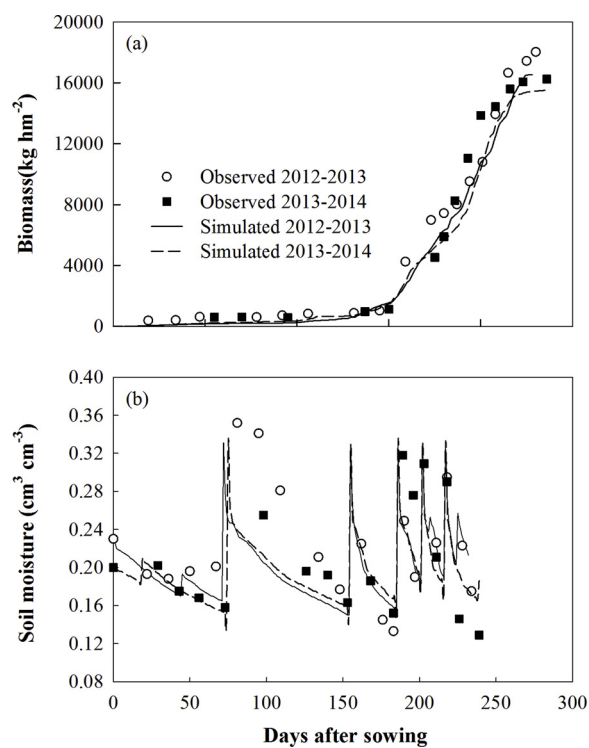


Fig. 6. Dynamics of biomass (a) and soil moisture at 0–20 cm layer (b) of winter wheat growth under sufficient irrigation (CK treatment) in the 2012–2013 and 2013–2014 growing seasons. The simulations were obtained based on indirectly measured soil parameters and GLUE-estimated genetic coefficients.

winter wheat. Field observations showed that soil water stress during wintering or returning green stage led to a decrease both in plant height and biomass. This indicated that serious and continuous water stress at early vegetative stages could heavily reduce aboveground biomass of winter wheat, which could not even be offset by later irrigations. Thus, an irrigation at the wintering or returning green stage could alleviate the inhibition of water stress on plant growth and increase plant height and aboveground biomass of winter wheat in the Guanzhong Plain of China. Different irrigation scenarios showed remarkable influences on the phenology of winter wheat, especially after the jointing stage. Low irrigation level could advance the maturity date up to three days. Earlier and more serious soil water stress would advance winter wheat phenology even more, which was consistent with the finding by [Mavromatis \(2014\)](#).

Winter wheat grain yields depends on the grain number and on the remobilization of the pre-flowering reserve as well as on the photosynthesis occurring during the grain filling period ([Artru et al., 2018](#); [Bijanazadeh and Emam, 2010](#)). Meanwhile, the dependent factors could be influenced by irrigation depth, water stress period, and their interaction. Both under irrigation levels of I1 and I2, soil water stress could heavily influence productive ears, grains per ear, unit grain weight, and final grain yield. Continuous water stress at both wintering and returning green stages (I1D1) led to a very low grain yield. When continuous water stress occurred at jointing and heading stages (I1D3), the highest grain yield was obtained since irrigations before jointing could guarantee the normal growth of winter wheat. However, unit grain weight was relatively low since water stress negatively influenced the early process of grain filling.

The treatment I2D2 (water stress at returning green and jointing stages) obtained the highest yield because of sufficient irrigation at wintering stage to meet the crop water requirements of vegetative growth. Two more irrigations at heading and grain-filling stages increased the number of productive ears, grains per ear, and unit grain

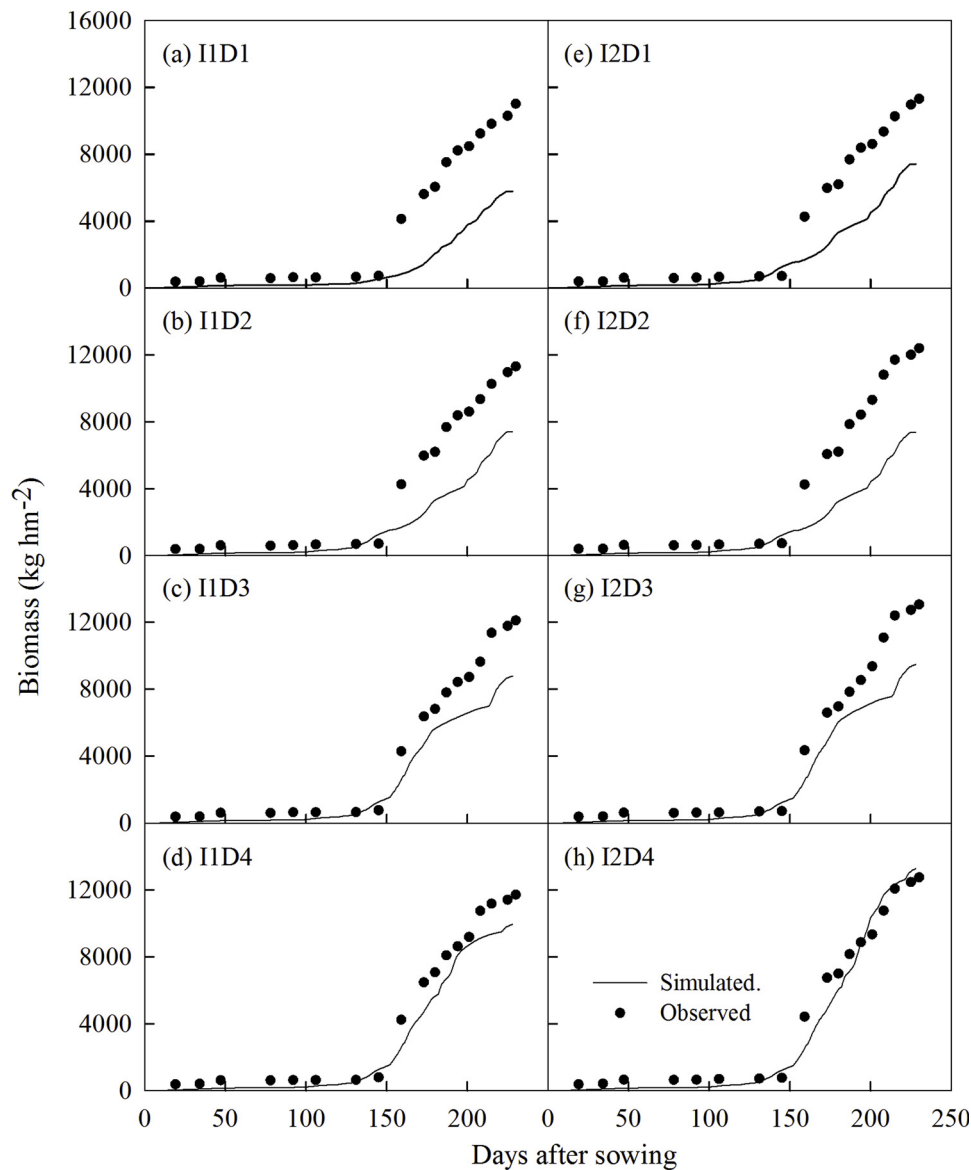


Fig. 7. Dynamic changes of biomass of winter wheat under different irrigation scenarios in the 2012–2013 growing seasons. The simulations were obtained based on indirectly measured soil parameters and GLUE-estimated genetic coefficients.

weight. This was different with the research which found that moderate water deficit during grain filling resulting in greater grain yield (Zhang et al., 2008). Generally, an irrigation at jointing could obviously increase productive ears, while irrigations at heading and grain-filling could markedly increase grains per ear and unit gain weight, which was consistent with the study done by Bakhsh et al. (2013).

In this study, we found returning-green was the critical stage for winter wheat irrigation. However, some other studies showed that the critical period of water requirement of winter wheat was from jointing to heading (Ji et al., 2014; Thorp, 2007). The difference was mainly because previous studies were performed in open fields where rainfall could confound the results due to additional unintended water input. However, this current study was conducted strictly under rainfall shelter almost without any precipitation input. Thus, soil moisture before sowing became very low and the influence of irrigation at early vegetative stage increased obviously. Winter wheat plants suffered longtime soil water stress in the treatments without irrigation at seedling (from emergence to jointing). The crop could not recover its normal growth even with sufficient irrigation at later stages and finally had very poor yields. This confirmed once again that irrigation at returning

green stage was crucial for a stable grain yield of winter wheat.

4.2. Influences of soil parameters related to water holding capacity on simulation accuracy

Although we found that there were only some small differences between initial indirectly measured and new manually tuned values of soil parameters of permanent wilting point (Table 4), the simulation accuracies of soil water contents were improved greatly in this study after using the manually tuned soil parameters instead (Fig. 9). This also resulted in higher simulation accuracies for total water storage and biomass (Figs. 10 and 11). Therefore, it could be concluded that soil parameters related to soil water holding capacity (i.e. permanent wilting point) played a very important role in simulating winter wheat growth under soil water stress conditions.

However, permanent wilting point is very difficult to be measured directly in practice. It is more functionally defined as the point at which plants wilt and do not recover overnight (Taiz and Zeiger, 1991). Crop species, soil type, and crop stage of growth all can affect the measured values of permanent wilting point (Norton and Silvertooth, 1998).

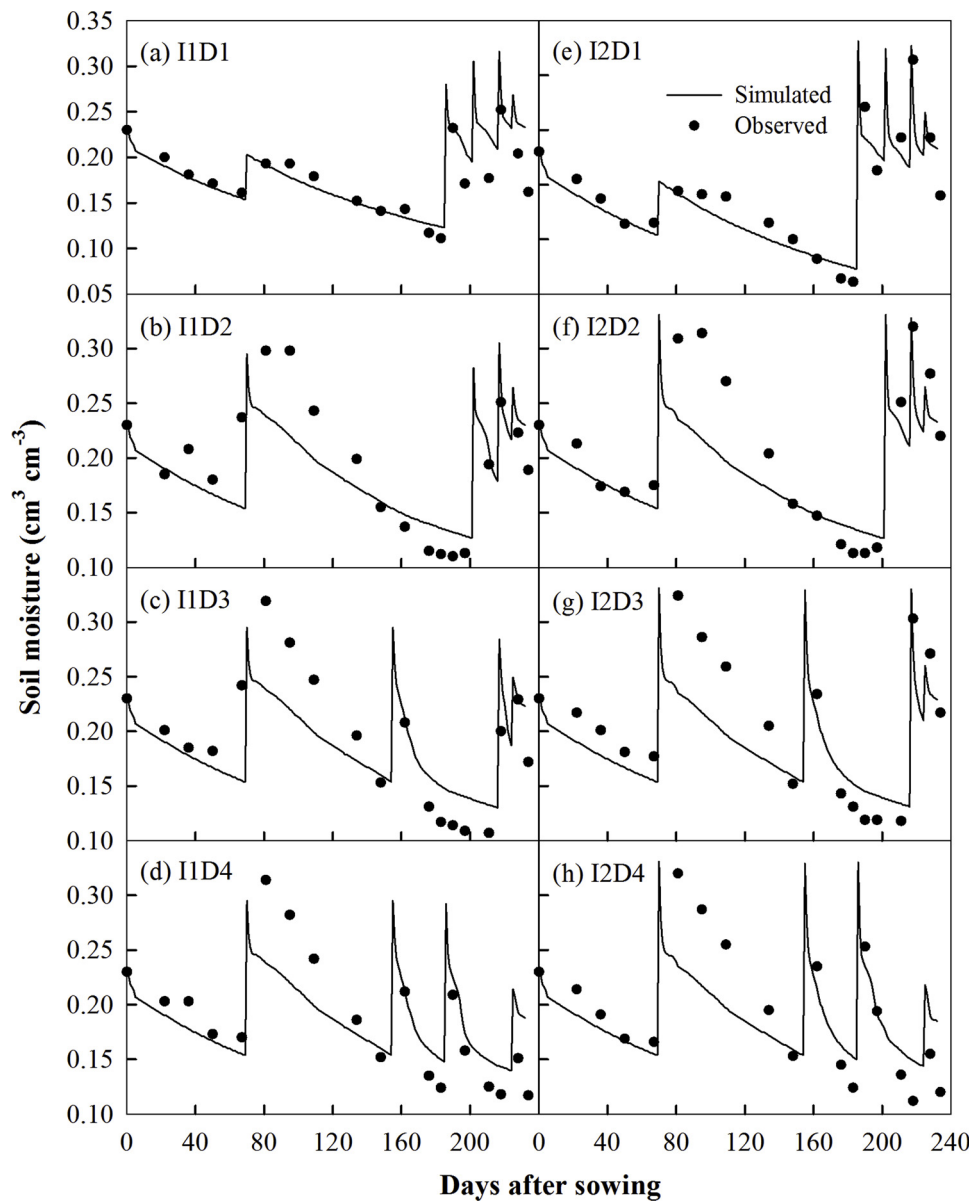


Fig. 8. Dynamic changes of soil moisture at the 0–20 cm layer for winter wheat growth under different irrigation scenarios in the 2012–2013 growing seasons. The simulations were obtained based on indirectly measured soil parameters and GLUE-estimated genetic coefficients.

Although permanent wilting point can be measured by some indirect methods, this would bring large uncertainty in parameter value and finally introduce large simulation errors.

Due to the uncertainties in indirectly measured values of permanent wilting point, simulated plant available soil water, which was defined as the difference between field capacity and permanent wilting point, was also uncertain. Thus, there could be some big errors in simulated biomass and yields caused only by some small differences in the values of relevant soil parameters. Generally, we suggested that the soil parameters related to water holding capacity played a very important role in simulating winter wheat growth when under severe soil water stress. Hence, these soil parameters should be measured more directly and accurately and need to be further tuned based on field observations when simulating crop growth under serious water stress conditions.

4.3. Evaluation of the CERES-Wheat model in arid conditions

Generally, the CERES-Wheat model was able to correctly simulate the growth and yield of winter wheat with sufficient water supply and

the simulation accuracy was relatively high, which was in agreement with some previous studies (Dettori et al., 2011; Langensiepen et al., 2008; Pecetti and Hollington, 1997; Thorp et al., 2010). However, when there were different scenarios of soil water stress, the simulation accuracy would change a lot for phenology, unit grain weight, above-ground biomass, and grain yield. When water stress occurred at the early vegetative stage, the simulation accuracy of the CERES-Wheat model became low. It usually simulated phenology dates earlier and overestimated unit grain weight, but underestimated final biomass and grain yield. At the same time, it also underestimated the soil moisture at the early growth stages, which was probably one of the main reasons for the low simulated biomass and grain yield. When water stress occurred at later growth stages, the simulation accuracy of the CERES-Wheat model improved a lot, but still had some kinds of errors. For example, for treatments related to D4 (water stress at heading and grain-filling stages) in the 2013–2014 season, the model seriously underestimated the unit grain weight of winter wheat (RMAE > 40%) either under irrigation level I1 or I2. In general, the CERES-Wheat model could simulate winter wheat growth with water stress at later

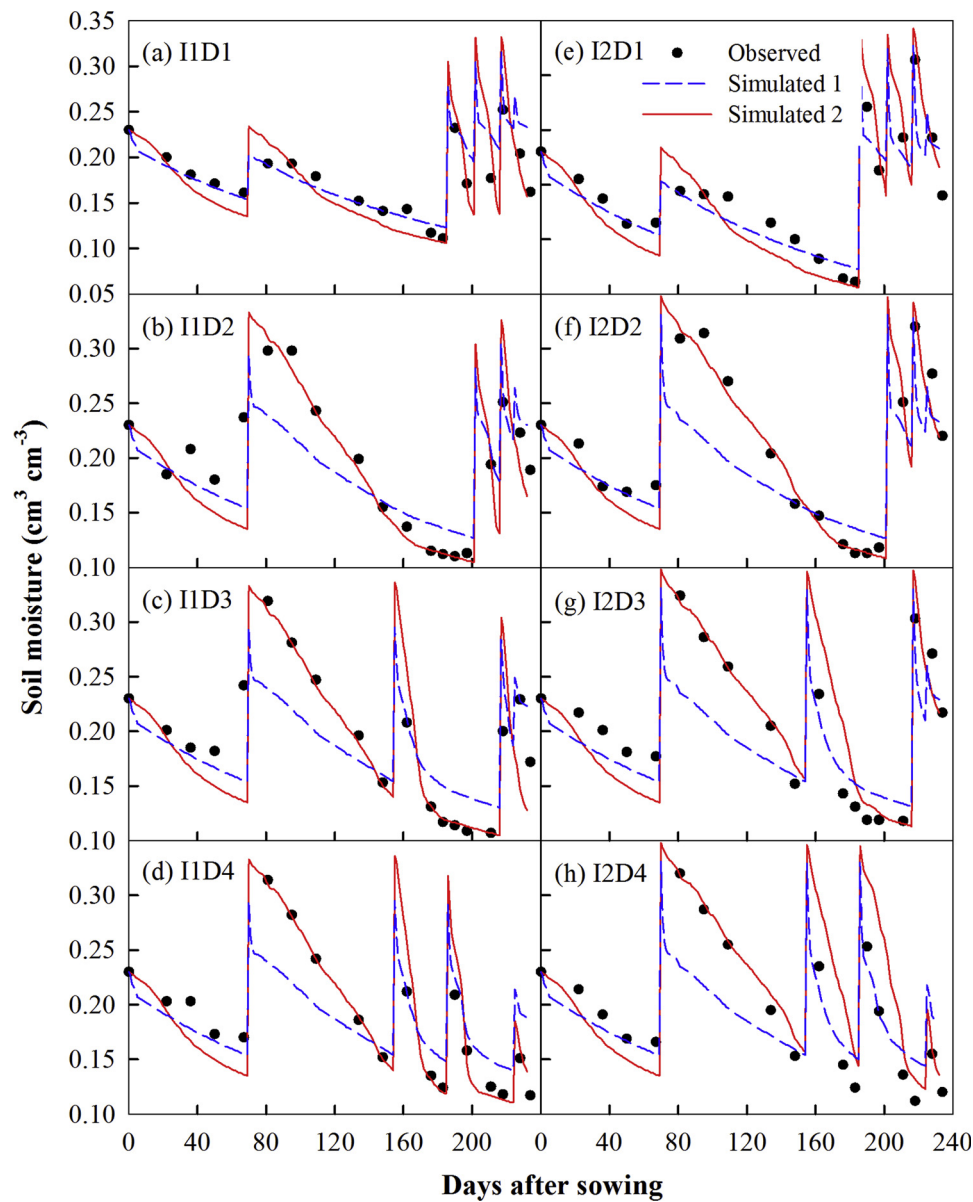


Fig. 9. Dynamic changes of soil moisture at the 0–20 cm layer for winter wheat growth under different irrigation scenarios in the 2012–2013 growing seasons. Simulated 1 indicates the simulation results obtained based on initial indirectly measured soil parameters and GLUE-estimated genetic coefficients, while Simulated 2 indicates the simulation results obtained based on the new manually tuned soil parameters and GLUE-estimated genetic coefficients.

growth stages more accurately than the growth with water stress at early stages.

Different reasons might contribute to such kind of simulation errors. Nouna et al. (2003) explored the reasons for the low accuracy of CERES-Wheat model under water stress. First, they found the model did not sufficiently simulate leaf area index (LAI) in the whole season; next, the water stress index calculated in the model did not consider the actual situation in field experiments. Dejonge et al. (2012) suggested that the simulation accuracy of evapotranspiration (ET) should be increased first if the CERES series models should be improved to simulate crop growth under water stress since the water stress indices in the model were directly related to ET values. While previous methods for evaluating ET using a static crop coefficient have worked well for studies under non-stressed water conditions, few studies have emphasized ET accumulation under water stress. Therefore, they provided a new equation that calculates a dynamic crop coefficient as a function of LAI.

In addition, some studies found that moderate water stress could stimulate the growth of roots of wheat seedling and increase the root-

shoot ratio, whereas serious water stress could inhibit root growth and decrease root activity (Sun et al., 2003). In some treatments of this study, water stress continuously occurred at wintering and returning green stages. Longtime water stress seriously retarded the growth of wheat roots. Thus, we suggest that an additional water stress index should be added in the CERES-Wheat model to take account of the complicated relationship between water stress and root growth and to improve the simulation accuracy of wheat growth under water stress at seedling stage.

The CERES-Wheat model gave the same simulations of anthesis and maturity dates for different irrigation scenarios, which contradicted the observations. In other words, the current CERES-Wheat model was unable to simulate the phenology discrepancy caused by soil water stress. This was because the phenology simulation in the current model was mainly based on meteorological factors, such as temperature and photoperiod, without consideration of the secondary influence of water and nutrient stress (Mcmaster et al., 2008). Additionally, Travasso and Delecolle (1995) pointed out that current CERES-Wheat model used air

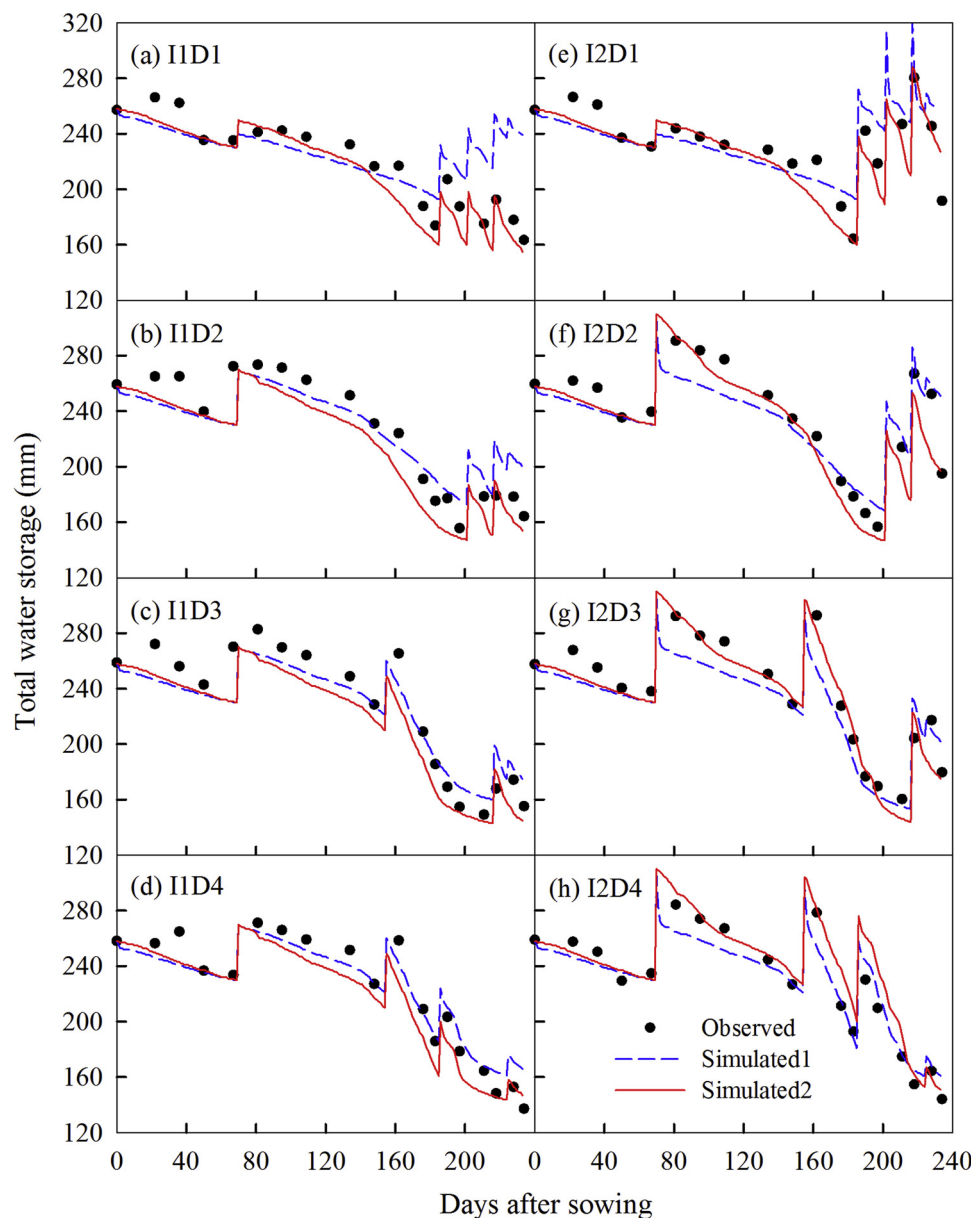


Fig. 10. Dynamic changes of total water storage in the 0–100 cm soil profile for winter wheat growth under different irrigation scenarios in the 2012–2013 growing season. Simulated 1 indicates the simulation results obtained based on initial indirectly measured soil parameters and GLUE-estimated genetic coefficients, while Simulated 2 indicates the simulation results obtained based on the new manually tuned soil parameters and GLUE-estimated genetic coefficients.

temperature in phenology prediction, rather than actual temperature in crop canopy. In general, the current CERES-Wheat model had some drawbacks in phenology prediction for winter wheat growth under serious water stress.

5. Conclusions

The experimental results showed that irrigation before jointing was necessary to reduce the inhibition of water stress on plant growth to guarantee higher plant height and aboveground biomass. Serious and early water stress could advance the phenology dates of winter wheat. The returning green and grain-filling stages were proved to be critical periods for field water management.

Generally, the CERES-Wheat model could simulate winter wheat growth under water stress at later reproductive stages better than the growth under water stress before jointing stages. The current CERES-Wheat model was not able to simulate the phenology discrepancies caused by different water stress scenarios.

The simulation accuracies of dynamics of water contents in 0–20 cm soil layer and winter wheat biomass all improved greatly after manually tuning the initially indirectly measured soil value of permanent wilting point. Generally, soil parameters related to soil water holding capacity played an important role in simulating winter wheat growth under severe soil water stress.

In general, the CERES-Wheat model proved to have some drawbacks to simulate winter wheat growth under complicated scenarios of soil water stress. To be effectively applied in winter wheat management in arid and semi-arid regions of China, we suggest the current CERES-Wheat model should be further validated, modified, and improved. The influences on winter wheat growth by water stress at seedling stages must be well understood and quantified, especially the influences on root system. Additionally, the secondary influence of water stress on wheat phenology should also be considered in the new phenology algorithm.

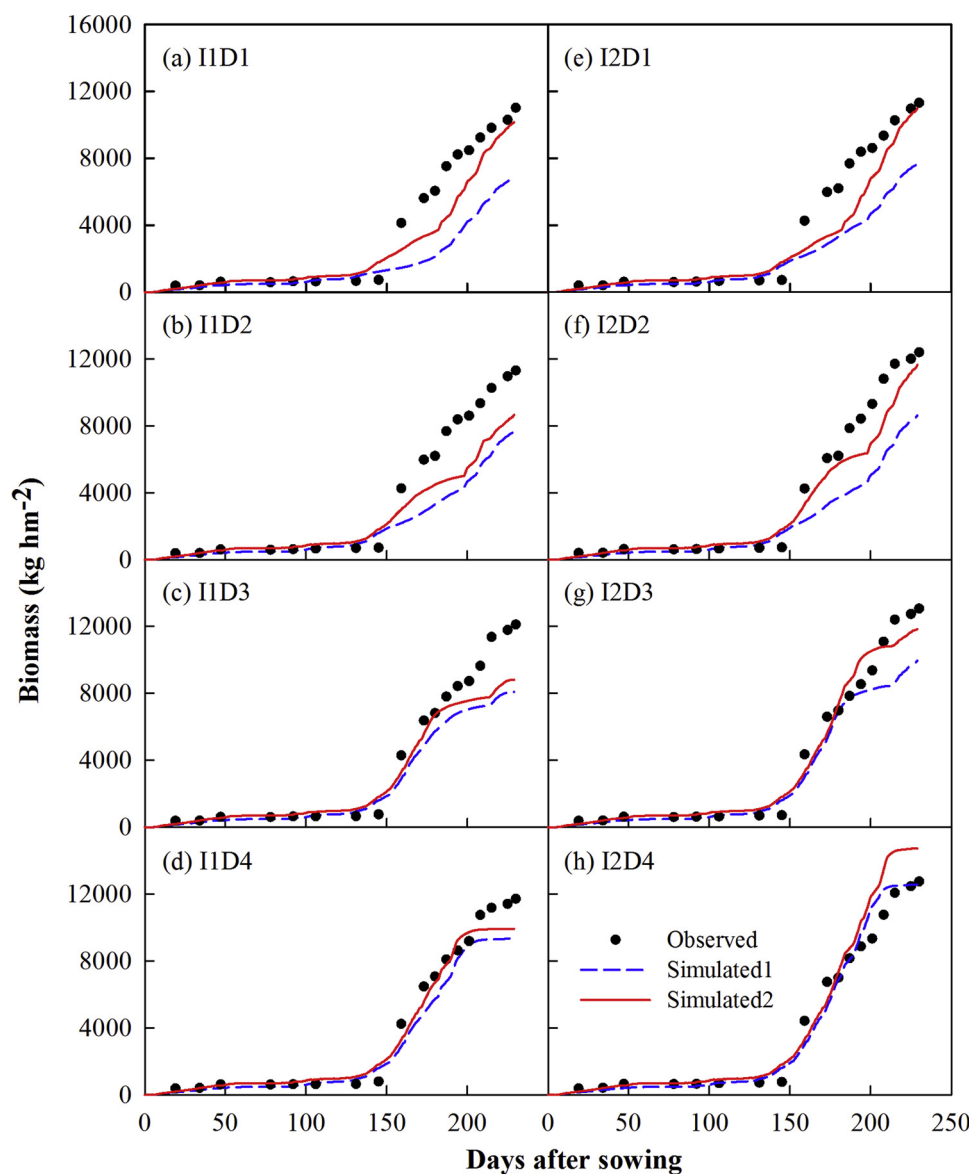


Fig. 11. Dynamic changes of biomass of winter wheat under different irrigation scenarios in the 2012–2013 growing seasons. Simulated 1 indicates the simulation results obtained based on initial indirectly measured soil parameters and GLUE-estimated genetic coefficients, while Simulated 2 indicates the simulation results obtained based on the new manually tuned soil parameters and GLUE-estimated genetic coefficients.

Declaration of Competing Interest

The authors declare that they have no known competing financial interests or personal relationships that could have appeared to influence the work reported in this paper.

Acknowledgements

This research was partially supported by the Natural Science Foundation of China (No. 4173064), the “Open Project Fund” from the State Key Laboratory of Soil Erosion and Dryland Farming on the Loess Plateau, Institute of Water and Soil Conservation, Chinese Academy of Sciences and Ministry of Water Resources (No. A314021402-1611), the Key Research and Development Program of Shaanxi (No. 2019ZDLNY07-03), the Science Promotion Project of Test and Demonstration Stations in the Northwest A&F University (TGZX2018-32), and the “111 Project” (No. B12007) of China.

References

- Allen, R.G., Pereira, L.S., Raes, D., Smith, M., 1998. Crop Evapotranspiration-guidelines for Computing Crop Water Requirements, FAO Irrigation and Drainage Paper 56. FAO, Roma, Italia.
- Anapalli, S.S., Ahuja, L.R., Ma, L., Timlin, D.J., Stockle, C.O., Boote, K.J., Hoogenboom, G., 2008. Current Water deficit stress simulations in selected agricultural system simulation models. In: Ahuja, L.R., Reddy, V.R., Saseendran, S.A., Yu, Q. (Eds.), Response of Crops to Limited Water: Understanding and Modeling Water Stress Effects on Plant Growth Processes. American Society of Agronomy, Crop Science Society of America, Soil Science Society of America, Madison, WI, pp. 1–38.
- Angstrom, A., 1924. Solar and terrestrial radiation. Report to the international commission for solar research on actinometric investigations of solar and atmospheric radiation. *Q. J. R. Meteorol. Soc.* 50, 121–126.
- Angus, J., Moncur, M., 1977. Water stress and phenology in wheat. *Crop Pasture Sci.* 28, 177–181.
- Antle, J.M., Basso, B., Conant, R.T., Hcj, G., Jones, J.W., Herrero, M., Howitt, R.E., Keating, B.A., Munozcarpena, R., Rosenzweig, C., 2016. Towards a new generation of agricultural system data, models and knowledge products: design and improvement. *Agric. Syst.* 155, 255–268.
- Artru, S., Dumont, B., Ruget, F., Launay, M., Ripoche, D., Lassois, L., Garré, S., 2018. How does STICS crop model simulate crop growth and productivity under shade conditions? *Field Crops Res.* 215, 83–93.
- Attia, A., Rajan, N., Xue, Q., Nair, S., Ibrahim, A., Hays, D., 2016. Application of DSSAT-CERES-Wheat model to simulate winter wheat response to irrigation management in

- the Texas High Plains. *Agric. Water Manag.* 165, 50–60.
- Bakhsh, A., Bashir, I., Farid, H.U., Wajid, S.A., 2013. Using cereals-wheat model to simulate grain yield production function for faisalabad, pakistan, conditions. *Exp. Agric.* 49, 461–475.
- Beven, K., Binley, A., 1992. The future of distributed models—model calibration and uncertainty prediction. *Hydrol. Process.* 6, 279–298.
- Biernath, C., Gayler, S., Bittner, S., Klein, C., Högy, P., Fangmeier, A., Priesack, E., 2011. Evaluating the ability of four crop models to predict different environmental impacts on spring wheat grown in open-top chambers. *Eur. J. Agron.* 35, 71–82.
- Bijanzadeh, E., Emam, Y., 2010. Effect of source-sink manipulation on yield components and photosynthetic characteristic of wheat cultivars (*Triticum aestivum* and *T. Durum* L.). *J. Appl. Sci.* 10, 564–569.
- Brisson, N., Mary, B., Ripoche, D., Jeuffroy, M.H., Ruget, F., Nicoulaud, B., Gate, P., Devienne-Barret, F., Antonioletti, R., Duru, C., 1998. STICS: a generic model for the simulation of crops and their water and nitrogen balances. I. Theory and parameterization applied to wheat and corn. *Agronomie* 18, 311–346.
- Cakir, R., 2004. Effect of water stress at different development stages on vegetative and reproductive growth of corn. *Field Crops Res.* 89, 1–16.
- Campos, I., Balbontin, C., González-Piqueras, J., González-Dugo, M.P., Neale, C.M.U., Calera, A., 2016. Combining a water balance model with evapotranspiration measurements to estimate total available soil water in irrigated and rainfed vineyards. *Agric. Water Manag.* 165, 141–152.
- Dejongs, K.C., Andales, A.A., Ascough, J.C., Hansen, N.C., 2011. Modeling of full and limited irrigation scenarios for corn in a semiarid environment. *Equine Vet. Educ.* 54, 481–492.
- Dejongs, K.C., Ji, J.C.A., Andales, A.A., Hansen, N.C., Garcia, L.A., Arabi, M., 2012. Improving evapotranspiration simulations in the CERES-Maize model under limited irrigation. *Agric. Water Manag.* 115, 92–103.
- Dettoni, M., Cesaraccio, C., Motroni, A., Spano, D., Duce, P., 2011. Using CERES-Wheat to simulate durum wheat production and phenology in Southern Sardinia, Italy. *Field Crops Res.* 120, 179–188.
- Eitzinger, J., Trnka, M., Hösch, J., Žalud, Z., Dubrovský, M., 2004. Comparison of CERES, WOFOST and SWAP models in simulating soil water content during growing season under different soil conditions. *Ecol. Modell.* 171, 223–246.
- Ghorbani, M.A., Shamshirband, S., Zare Haghi, D., Azani, A., Bonakdari, H., Ebtehaj, I., 2017. Application of firefly algorithm-based support vector machines for prediction of field capacity and permanent wilting point. *Soil Tillage Res.* 172, 32–38.
- Hammer, G., Cooper, M.F., Welch, S., Walsh, B., Van, E.F., Chapman, S., Podlich, D., 2006. Models for navigating biological complexity in breeding improved crop plants. *Trends Plant Sci.* 11, 587–593.
- He, J., 2008. Best Management Practice Development With the CERES-Maize Model for Sweet Corn Production in North Florida. Agricultural and Biological Engineering Department. University of Florida, Gainesville, FL.
- He, J., 2009. Applying glue for estimating CERES-Maize genetic and soil parameters for sweet corn production. *Trans. Asabe* 52, 1907–1921.
- He, J., Cai, H., Bai, J., 2013. Irrigation scheduling based on CERES-Wheat model for spring wheat production in the Minqin Oasis in Northwest China. *Agric. Water Manag.* 128, 19–31.
- He, J., Jones, J.W., Graham, W.D., Dukes, M.D., 2010. Influence of likelihood function choice for estimating crop model parameters using the generalized likelihood uncertainty estimation method. *Agric. Syst.* 103, 256–264.
- Jamieson, P.D., Porter, J.R., Goudriaan, J., Ritchie, J.T., Hvan, K., Stol, W., 1998. A comparison of the models AFRCWHEAT2, CERES-Wheat, Sirius, SUCROS2 and SWHEAT with measurements from wheat grown under drought. *Field Crops Res.* 55, 23–44.
- Ji, J., Cai, H., He, J., Wang, H., 2014. Performance evaluation of CERES-Wheat model in Guanzhong Plain of Northwest China. *Agric. Water Manag.* 144, 1–10.
- Jones, J.W., Antle, J.M., Basso, B., Boote, K.J., Conant, R.T., Foster, I., Godfray, H.C.J., Herrero, M., Howitt, R.E., Janssen, S., 2016. Brief history of agricultural systems modeling. *Agric. Syst.* 155, 240–254.
- Jones, J.W., Hoogenboom, G., Porter, C.H., Boote, K.J., Batchelor, W.D., Hunt, L.A., Wilkens, P.W., Singh, U., Gijsman, A.J., Ritchie, J.T., 2003. The DSSAT cropping system model. *Eur. J. Agron.* 18, 235–265.
- Kang, S., Zhang, L., Liang, Y., Hu, X., Cai, H., Gu, B., 2002. Effects of limited irrigation on yield and water use efficiency of winter wheat in the Loess Plateau of China. *Agric. Water Manag.* 55, 203–216.
- Langensiepen, M., Hanus, H., Schoop, P., Gräsele, W., 2008. Validating CERES-wheat under North-German environmental conditions. *Agric. Syst.* 97, 34–47.
- Mavromatis, T., 2014. Pre-season prediction of regional rainfed wheat yield in Northern Greece with CERES-Wheat. *Theor. Appl. Climatol.* 117, 653–665.
- McMaster, G.S., White, J.W., Weiss, A., Baenziger, P.S., Wilhelm, W.W., Porter, J.R., Jamieson, P.D., 2008. Simulating crop phenological responses to Water deficits. In: Ahuja, L.R., Reddy, V.R., Saseendran, S.A., Yu, Q. (Eds.), *Response of Crops to Limited Water: Understanding and Modeling Water Stress Effects on Plant Growth Processes*. Advances in Agricultural Systems Modeling Series 1, ASA, CSSA, SSSA, 5585 Guilford Road, Madison, WI 53711-5801, USA.
- McMaster, G.S., Wilhelm, W.W., 2003. Phenological responses of wheat and barley to water and temperature: improving simulation models. *J. Agric. Sci.* 141, 129–147.
- Minasny, B., McBratney, A.B., Bristow, K.L., 1999. Comparison of different approaches to the development of pedotransfer functions for water-retention curves. *Geoderma* 93, 225–253.
- Mohanty, M., Sinha, N.K., Painuli, D.K., Bandyopadhyay, K.K., Hati, K.M., Sammi Reddy, K., Chaudhary, R.S., 2015. Modelling soil water contents at field capacity and permanent wilting point using artificial neural network for indian soils. *Natl. Acad. Sci. Lett.* 38, 373–377.
- Norton, E.R., Silvertooth, J.C., 1998. Field determination of permanent wilting point. In: Silvertooth, J.C. (Ed.), *Cotton. a College of Agriculture Report Series P-112*, pp. 230–237.
- Nouna, B.B., Katerji, N., Mastrotrilli, M., 2003. Using the CERES-Maize model in a semi-arid Mediterranean environment. New modelling of leaf area and water stress functions. *Eur. J. Agron.* 19, 115–123.
- Pachepsky, Y.A., Timlin, D., Varallyay, G., 1996. Artificial neural networks to estimate soil water retention from easily measurable data. *Soil Sci. Soc. Am. J.* 60, 727–733.
- Pecetti, L., Hollington, P.A., 1997. Application of the CERES-wheat simulation model to durum wheat in two diverse Mediterranean environments. *Eur. J. Agron.* 6, 125–139.
- Porter, J.R., Jamieson, P.D., Wilson, D.R., 1993. Comparison of the wheat simulation models AFRCWHEAT2, Ceres -wheat and Swheat for non-limiting conditions of crop growth. *Field Crops Res.* 33, 131–157.
- Priestley, C.H.B., Taylor, R.J., 1972. On the assessment of surface heat flux and evaporation using large-scale parameters. *Mon. Weather. Rev.* 100, 81–92.
- Rab, M.A., Chandra, S., Fisher, P.D., Robinson, N.J., Kitching, M., Aumann, C.D., Imhof, M., 2011. Modelling and prediction of soil water contents at field capacity and permanent wilting point of dryland cropping soils. *Soil Res.* 49, 389–407.
- Ritchie, J.R., Otter, S., 1985. Description and performance of CERES-Wheat: a user-oriented wheat yield model. *US Department of Agriculture, ARS* 38, 159–175.
- Ritchie, J.T., 1985. A User-Oriented Model of the Soil Water Balance in Wheat. Springer US.
- Ritchie, J.T., 1998. Soil Water balance and plant Water stress. In: Tsuji, Y.G., Hoogenboom, G., Thornton, P.K. (Eds.), *Understanding Options for Agricultural Production*. Kluwer Academic Publishers, Dordrecht, pp. 79–98.
- Ritchie, J.T., Singh, U., Godwin, D.C., Bowen, W.T., 1998. Cereal growth, development and yield. In: Tsuji, Y.G., Hoogenboom, G., Thornton, P.K. (Eds.), *Understanding Options for Agricultural Production*. Kluwer Academic Publishers, Dordrecht, pp. 79–98.
- Romanowicz, R.J., Beven, K.J., 2006. Comments on generalised likelihood uncertainty estimation. *Reliab. Eng. Syst. Saf.* 91, 1315–1321.
- Scheinost, A.C., Sinowski, W., Auerswald, K., 1997. Regionalization of soil water retention curves in a highly variable soilscape, I. Developing a new pedotransfer function. *Geoderma* 78, 129–143.
- Shan, L., Deng, X., Kang, S., 2002. Current situation and perspective of agricultural water used in semiarid area of China. *J. Hydraul. Eng.* 33, 27–31 (In Chinese with English abstract).
- Sun, C., Bai, S., Bai, B., 2003. Effect of water stress on root growth and physiological characters of wheat seedlings. *Journal of Jilin Agricultural University* 25, 485–489 (In Chinese with English abstract).
- Taiz, L., Zeiger, E., 1991. *Plant Physiology*. The Benjamin/Cummings Publishing Co., Inc, Redwood City, CA.
- Thorp, K.R., 2007. Using cross-validation to evaluate CERES-Maize yield simulations within a decision support system for precision agriculture. *Trans. Asabe* 50, 1467–1479.
- Thorp, K.R., Hunsaker, D.J., French, A.N., White, J.W., Clarke, T.R., Pinter Jr., P.J., 2010. Evaluation of the CSM-CROPSIM-CERES-Wheat model as a tool for crop water management. *Trans. Asabe* 53, 87–102.
- Travasso, M.I., Delecolle, R., 1995. Adaptation of the CERES-wheat model for large area yield estimation in Argentina. *Eur. J. Agron.* 4, 347–353.
- van Genuchten, M.T., 1980v. A closed-form equation for predicting the hydraulic conductivity of unsaturated soils I. *Soil Sci. Soc. Am. J.* 44, 892–898.
- van Keulen, H., Seligman, N.G., 1987v. Simulation of Water Use, Nitrogen Nutrition and Growth of a Spring Wheat Crop. *Simulation Monographs*, Pudoc, Wageningen.
- van Laar, H.H., Goudriaan, J., van Keulen, H., 1992v. Simulation of Crop Growth for Potential and Water, *Simulation Reports CABO-TT, 27, CABO-DLO/TPE-WAU*. Wageningen.
- Wang, C.Y., Guo, T.C., Peng, Y., Zhu, Y.J., Ma, D.Y., Zhang, C.J., 2004. Effects of post-anthesis irrigation on grain quality indices and yield in winter wheat (*Triticum aestivum* L.). *Acta Agron. Sin.* 30, 1031–1035 (In Chinese with English abstract).
- Wang, S., Zhang, X., Pei, D., 2006. Impacts of different water supplied conditions on root distribution, yield and water utilization efficiency of winter wheat. *Transactions of the Chinese Society of Agricultural Engineering (Transactions of the CSAE)* 22, 27–32 (In Chinese with English abstract).
- Wösten, J.H.M., Finke, P.A., Jansen, M.J.W., 1995. Comparison of class and continuous pedotransfer functions to generate soil hydraulic characteristics. *Geoderma* 66, 227–237.
- Zadoks, J.C., Chang, T.T., Konzak, C.F., 1974. A decimal code for the growth stages of cereals. *Weed Res.* 14, 415–421.
- Zhang, X., Chen, S., Sun, H., Pei, D., Wang, Y., 2008. Dry matter, harvest index, grain yield and water use efficiency as affected by water supply in winter wheat. *Irrig. Sci.* 27, 1–10.